The Journal of Experimental Biology 211, 2876-2888
Published by The Company of Biologists 2008
doi:10.1242/jeb.018515

Hydrozoan nematocytes send and receive synaptic signals induced by mechano-chemical stimuli

Dominik Oliver*, Martin Brinkmann†, Thiemo Sieger‡ and Ulrich Thurm§

Institute for Neurobiology and Behavioral Biology, University of Münster, Badestr. 9, D-48149 Münster, Germany

*Present address: Institute for Physiology and Pathophysiology, Department of Neurophysiology, University of Marburg, Deutschhausstrasse 2, D-35037 Marburg, Germany

†Present address: Smiths Medical International, Nottulnerstrasse 25, D-48249 Buldern, Germany

‡Present address: Tyska Skolan, Karlavägen 25, S-11431 Stockholm, Sweden

§Author for correspondence (e-mail: thurmu@uni-muenster.de)

Accepted 30 June 2008

SUMMARY

Nematocytes, the stinging cells of Hydrozoa, can be considered as prototypic mechanosensory hair cells bearing a concentric hair bundle, the cnidocil apparatus. These cells produce typical mechanoreceptor potentials in response to deflection of their cnidocil. Here we show that mechanosensory signals are relayed to neighbouring nematocytes *via* chemical neurotransmission and that nematocytes receive synaptic input from surrounding nematocytes, hair cells and probably from epithelial cells. Intracellular voltage recordings from stenotele nematocytes of capitate hydroid polyps showed two distinct types of responses when other nematocytes within the same tentacle were mechanically stimulated: (i) graded depolarizations of variable duration ('L-potentials'), and (ii) uniform impulse-like, often repetitive depolarizations ('T-potentials') that occurred in correlation with contractions of epitheliomuscular cells. Voltage clamp experiments showed that despite the stereotyped time course of T-potentials, their generation did not involve electrically excitable conductances. Instead, time course, post-stimulus delay, susceptibility to blockers of neurotransmission and gap junctions, and induction by electrical stimulation of other nematocytes indicate that L- and T-potentials are postsynaptic, most likely glutamatergic potentials. Both result from different presynaptic pathways: L-potentials are induced monosynaptically by presynaptic receptor potentials, T-potentials are most likely triggered by presynaptic action potentials propagating through the ectodermal epithelium *via* gap junctions. Moreover, contact-chemosensory (phospholipid) stimulation of the presynaptic nematocyte is a positive modulator of the nematocyte's afferent synaptic efficacy and of cnidocyst discharge, both triggered by mechanoreceptor potentials. The results reveal that hydrozoan nematocytes act as bimodal sensory cells, signalling coincident chemical and mechanical stimuli indicative of prey, and receive signals from other nematocytes and sensory cells.

Supplementary material available online at http://jeb.biologists.org/cgi/content/full/211/17/2888/DC1

Key words: cnidocyte, hair cell, mechanoreception, postsynaptic potential.

INTRODUCTION

Nematocytes, the stinging cells (cnidocytes) that characterize the phylum Cnidaria, have been viewed as highly specialized cells (for a review, see Tardent, 1995). However, more recent studies show that they may provide informative paradigms for a number of basic neurobiological mechanisms. The mechanosensory organelle of hydrozoan nematocytes is the cnidocil apparatus, a concentric hair bundle composed of a cilium and stereovilli originating from the same cell (in contrast to multicellular hair bundles of sea anemones). The cnidocil apparatus can be considered a prototype, as similar concentric hair bundles are found in mechanosensory hair cells of most invertebrate phyla, from cnidarians to lower chordates (Slautterback, 1967; Golz and Thurm, 1991; Golz, 1994; Thurm et al., 1998a; Holtmann and Thurm, 2001b). Sensory transduction in hydrozoan nematocytes shows mechanically controlled conductance changes similar to those of vertebrate hair cells but without directional selectivity (Brinkmann et al., 1996). Nematocyte receptor potentials drive the discharge of the cnidocyst, exhibiting a specialized form of exocytosis (Brinkmann et al., 1996; Gitter and Thurm, 1996; Nüchter et al., 2006). In hydrozoan stenotele nematocytes, the probability of cyst discharge is increased by contact-chemical stimuli acting at the shaft of the cnidocil thus providing a paradigm for the modulation of exocytotic processes (Thurm and Lawonn, 1990; Brinkmann et al., 1995; Thurm et al., 1998b; Thurm et al., 2004).

Originally, nematocytes were thought to be independent senso-effectors (Parker, 1916) with the cnidocil acting as the sensory organelle controlling the cnidocyst, the intracellular effector organelle. However, chemical stimuli have been known to change the sensitivity of nematocytes *via* distinct chemoreceptor cells in anthozoans (Pantin, 1942; Watson and Hessinger, 1989), suggesting intercellular communication. More recently, electrical responses have been recorded in hydrozoan nematocytes in response to water-soluble chemical stimuli and these responses were proposed to be postsynaptic (Purcell and Anderson, 1995; Price and Anderson, 2006). Similarly, we have observed that mechanical stimulation of cnidocils induces electrical responses in neighbouring nematocytes (Brinkmann, 1994; Brinkmann et al., 1995; Thurm et al., 1998b; Thurm et al., 2004), suggestive of synaptic signalling between nematocytes. This observation thus strongly challenges the concept of nematocytes as independent functional units. In fact, electron microscopy demonstrated efferent and afferent synaptic contacts at nematocytes (Westfall, 1996; Holtmann and Thurm, 2001a). Here

we provide a detailed electrophysiological analysis of the afferent and efferent signalling pathways activating hydrozoan nematocytes.

We investigated *Stauridiosarsia producta* and *Dipurena reesi*, both stolonial capitate Hydrozoa with large nematocytes. Additionally, we chose to study *Coryne tubulosa* as the smaller size of their tentacular spheres allowed for an electron-microscopical characterization of all cells and their connectivity within complete spheres (Holtmann and Thurm, 2001a; Holtmann and Thurm, 2001b). We show that hydrozoan stenotele nematocytes receive sensory signals from other nematocytes as well as from sensory cells. We demonstrate two types of stimulus-induced electrical events, both of which are generated *via* chemical synapses. These types differ in the origin and route of the presynaptic signals. The signals conveyed from other nematocytes disclose nematocytes to play a unique role as bimodal sensory cells detecting mechano-chemical stimuli indicative of prey. Consequently, nematocytes contribute substantially to the sensory input of hydrozoan tentacles. Together with sensory hair cells, they present an evolutionary primordial paradigm for afferent synaptic signal transmission.

MATERIALS AND METHODS

Stauridiosarsia producta (Wright; syn. *Sarsia producta*) and *Coryne tubulosa* (Sars; syn. *Sarsia tubulosa*) were obtained from the Biologische Anstalt Helgoland; *Dipurena reesi* (Vanucci; syn. *Sarsia reesi*) was a gift from Prof. V. Schmid, Zoological Institute Basel. Although all three species are classified as Corynidae, the hydroids of *D. reesi* are more similar to those of *Cladonema radiatum* belonging to the Cladonemidae (see Brinkmann and Petersen, 1960). All species were raised at our institute in artificial seawater at 14–16°C and fed with *Artemia* nauplia every 2–3 days. Data presented are from *Stauridiosarsia producta* unless indicated otherwise.

The tentacles of capitate Hydrozoa concentrate all nematocytes within their non-contractile terminal spheres (Fig. 1). Besides the nematocytes, which are exclusively of the stenotele type, the spheres comprise four types of sensory cells: mechanosensory hair cells with a long or short cilium, rootlet cells and vesicle-rich, probably chemosensory, cells (Holtmann and Thurm, 2001b). Somata of ganglion cells are absent in the spheres.

Methods have been described in detail before by Brinkmann et al. (Brinkmann et al., 1996). Briefly, tentacles were cut from relaxed polyps and held at the sphere by a suction capillary (Fig. 1). Since the residual shaft at the sphere moved spontaneously and in response to stimuli applied to the sphere, absence of contact with the capillary was essential to keep the cells to be studied at a stable position and allowed the observation of shaft movements. Sphere and shaft were continuously superfused through one of three capillaries (inner diameter ~1 mm) arranged concentrically such that the tentacular sphere was located at the intersection of their streams. The fluid flow (2–3 mm s^{-1}) was controlled by electromagnetic valves, yielding complete solution exchange within <1 s. Reference solution was artificial seawater (ASW; in mmol l^{-1}: NaCl 414, $MgCl_2$ 24, $MgSO_4$ 24, KCl 9, $CaCl_2$ 9, Hepes 1). To enable and accelerate penetration of agents into the tissue, DMSO was added in two experiments. The concentrations used (0.025–5%; v/v) had no effect on the sensitivity of nematocytes or on the parameters studied. All measurements were done at 20–24°C.

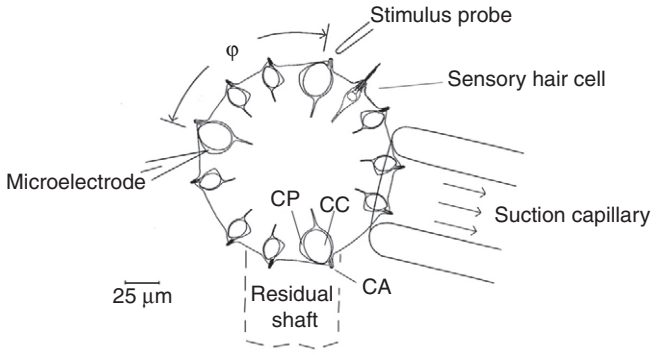

Fig. 1. Schematic diagram of an isolated capitate tentacle arranged for stimulation of a nematocyte or sensory hair cell and synchronous intracellular recording from a distant nematocyte. The tentacular sphere is held by a suction capillary. φ, angle between stimulated and recorded cells; CA, cnidocil apparatus; CC, cnidocyst; CP, cytoplasm of nematocyte.

During measurements, specimens were observed under a microscope with a ×40 or ×50 water immersion objective (NA 0.75 or 1.0) and Nomarski interference contrast optics. A video camera, video mixer and video recorder were used to synchronize the electrical recording with the microscopic image for on- and off-line evaluation.

For electrical measurements conventional microcapillaries filled with 1 mol l^{-1} KCl or LiCl (for combination with Lucifer Yellow) were used (20–60 MΩ). Intracellular voltage measurements were performed in a current clamp circuit, current measurements in a single-electrode voltage clamp circuit (switching between voltage measurement and current injection at 6–7.5 kHz; Sylgard-coated microcapillaries of reduced resistance: 8–15 MΩ). Errors in space clamping can be estimated to be <5% for the penetrated spherical soma and <20% for the stalk and neurites of the nematocytes (estimated length constants 700 µm and 200 µm, respectively (Fig. 1) (Holtmann and Thurm, 2001a). In some experiments penetrated cells were visualized by iontophoretic injection of Lucifer Yellow through the recording electrode [10 nA hyperpolarizing for 30 s (see Brinkmann et al., 1996)].

For mechanical stimulation of individual cnidocils and sensory hair bundles a glass probe (tip diameter 1–4 µm) was mounted onto a two-dimensional piezo-electric driver. Its stimulating movements were performed in the *x–y* plane and were opto-electronically controlled in two feedback loops. The tip of the probe, 30–100 µm long, was bent at a right angle to be aligned parallel with the optical axis. Thus, movements along the longitudinal axis of the probe in the *x–y* plane could be used, providing high stiffness and allowing for recording of tip movements with a time resolution of 10 µs [for time course of excursions see Brinkmann (Brinkmann et al., 1996); for influence of steepness of stimulation see Appendix]. The opto-electronic records obtained in the feedback control were calibrated and used in the figures as stimulus trace. In the resting state, the tip of the probe was usually not in contact with the cnidocil or hair bundle. Thus, the excursion of the latter was smaller than the recorded tip movement.

For contact-chemical stimulation of individual cnidocils, the tip of a glass probe (as above) was coated with L-α-phosphatidylcholine, dissolved in 1:1 chloroform:methanol (2 mg 10 ml^{-1}). The probe was dipped into this solution, then air-dried for ⩾30 s. During experiments, coating was repeated at least every 30 min.

For electrical stimulation of nematocytes, voltage impulses were applied by an extracellular capillary (5–15 µm diameter) filled with ASW. Its polished tip enclosed the apical area of a nematocyte without touching the cnidocil apparatus, thus avoiding mechanical stimulation. The capillary was pushed against the cell surface and negative pressure was applied to ensure close contact. Current was

thus fed transepithelially and focused at a single nematocyte. An apical anodic voltage impulse thus hyperpolarized the apical surface membrane and depolarized the basolateral membrane, the site of putative afferent synapses, and *vice versa* for a cathodic impulse. In some experiments the tip of the capillary was filled with a suspension of lecithin micelles.

RESULTS

Voltage responses caused by distant mechanical stimuli

In nematocytes of all three hydrozoan species studied, mechanical stimulation of distant cells of the tentacular sphere as well as spontaneous contractions of the tentacular shaft induced depolarizing voltage changes (Figs 2–4; see Fig. 1 for experimental configuration and definition of distance by angle φ). Mechanical or electrical stimulation of the recorded cell itself did not induce similar voltage changes. Corresponding to their different time courses, the voltage changes were classified as L (long)-potentials or T (transient)-potentials.

L-potentials

L-potentials were variable in duration, graded in peak amplitude, and often polyphasic (Fig. 2Bb) with overlapping potentials summating. The amplitude of L-potentials reached up to 44 mV, depolarizing the membrane up to –20 mV (supplementary material Table S1). Amplitude and duration of L-potentials exhibited weak correlation with amplitude and duration of the mechanical stimulus (data not shown). L-potentials were observed in response to the following stimuli.

(1) Deflections of the concentric hair bundle of a sensory hair cell of *Coryne* (Fig. 2A,B) induced an L-type response in 72% of tested pairs of nematocyte and hair cell (47 hair cells tested). In the larger spheres of *Stauridiosarsia* only four of 25 pairs showed these responses. Neither degree nor direction of the hair bundle deflection was reflected in the response amplitude (deflections of 3°–28°; Fig. 2B). Results were similar using an uncoated or lecithin-coated glass probe for hair bundle stimulation. Repetitive stimulation at 1–0.5 Hz induced 1–13 consecutive responses. After a recovery time of 50–200 s, responses could be evoked again stimulating the same hair cell. Within the recovery period, responses from the same recorded nematocyte could be evoked by stimulation of other hair cells. The shortest latency in response to hair deflection was 9 ms, however, latency increased with consecutive stimulations to up to 100 ms.

(2) Deflection of the cnidocil apparatus of a distant nematocyte induced L-potentials in the recorded nematocyte similar to those caused by stimulation of a sensory hair cell, but with a high variability in failure rate and in amplitude. The response depended on a contact-chemical component of stimulation and whether or not

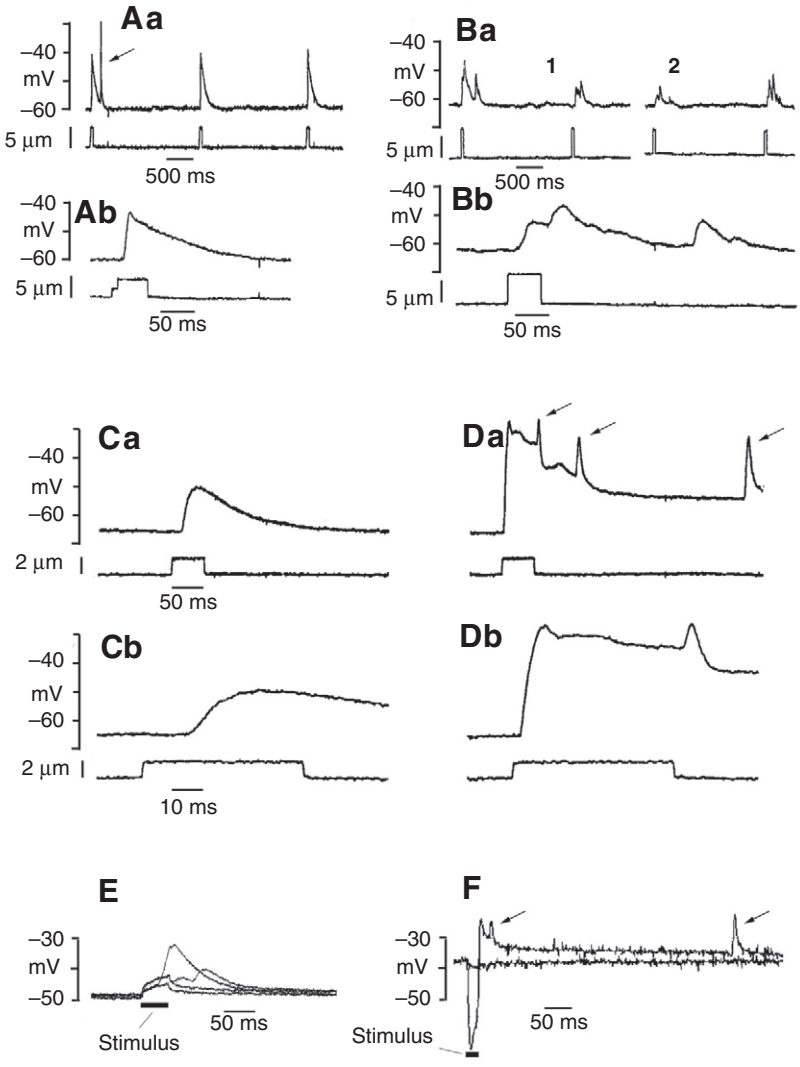

Fig. 2. L-potentials in nematocytes. Upper trace of each record: membrane voltage; lower trace: stimulatory excursion of the probe. (A,B) L-potentials induced by deflections of the hair bundle of a sensory hair cell at two different time scales (a,b). (A) in *Stauridiosarsia* hair deflection was 28°; a pre-impulse was used to guarantee synchronous starts of the probe and the hair at the second step. The first response in Aa is superimposed by a T-potential (arrow; see Fig. 4). (B) L-potentials in *Coryne* induced by hair deflection of +10° (Ba, 1) and –9° (opposite direction, Ba, 2). (C,D) L-potentials induced by deflections of the cnidocil apparatus of a distant nematocyte in *Stauridiosarsia;* responses from the same pair of cells in C and D; (C) without, (D) with discharge of the cnidocyst of the stimulated cell. The responses in Ca and Da are shown on an enlarged time scale in Cb and Db. Note shortening of latency of L-potential from 15 ms (C) to 2.6 ms (D). T-potentials are superimposed in D (arrows). (E,F) Responses of nematocytes of *Stauridiosarsia* to transepithelial electrical stimulation at the site of a distant nematocyte. The duration of the voltage step stimuli is indicated by a bar beneath the responses and is reflected in the recorded voltage by distorted rectangles. (E) Four superimposed responses to impulses (Stimulus) of equal duration with positive sign at the cell surface (depolarizing the basolateral membrane); two impulses were of 100 mV, 2 of 120 mV amplitude. One stimulus of each amplitude induced an L-potential; the highest was induced by a 100 mV impulse (latencies 20 and 48 ms). (F) Two superimposed responses to impulses with negative sign at the distant cell surface (depolarizing the apical membrane): the smaller impulse (–40 mV) did not induce a response; the larger (–60 mV) elicited the discharge of the stimulated nematocyte and induced a corresponding large L-potential (latency 10 ms) of long duration, superimposed by two T-potentials. (The small peak-amplitude of the L-potential corresponds to the small membrane voltage of the recorded cell. At the peak the membrane became depolarized to the usual range, about –25 mV, as found in D.)

the nematocyst of the stimulated cell discharged (Fig. 2C,D and Fig. 3A). 37% of purely mechanically stimulated distant nematocytes elicited L-potentials in the recorded nematocytes; 8% of the stimulated nematocytes discharged (recorded cells: *N*=13; stimulated cells: *N*=123). However, with a lecithin-coated probe, 86% of stimulated cells induced L-potentials and 67% of stimulated cells discharged. All discharging cells induced L-potentials (recorded cells: *N*=20; stimulated cells: *N*=249). Those responses that were associated with the discharge of the stimulated cell had a mean amplitude of 25.0±6.2 mV (± s.d.; *N*=146; range 10–44 mV) and latencies of 2.1±1.2 ms (86% of latencies between 0.6 ms and 3.0 ms; *N*=146; Fig. 3B).

The amplitudes of L-potentials that occurred without discharge of the stimulated cell, in contrast, varied between <1 mV and 24 mV (*N*=164) even for saturating stimuli, depending on the pre-stimulus history (see below). The latencies of these potentials varied between 2.6 ms and 45 ms (*N*=164) (Fig. 3A–C). A strict negative correlation between these latencies and amplitudes became evident when the responses from individual pairs of cells were compared, yielding correlation coefficients around –0.95 (Fig. 3C). Also the discharge-associated maximal amplitudes and minimal latencies fit this correlation in the individual pairs of cells. By contrast, when comparing discharge-associated responses of different pairs of cells, no correlation between amplitude and latency was found (coefficient 0.05; Fig. 3B).

When a given nematocyte was subjected to repeated stimulation at intervals <1 min, without inducing a discharge, the amplitude and latency of L-potentials recorded in a distant nematocyte usually decayed with repetitions (Fig. 3A). This decay was most prominent with purely mechanical stimulation. The number of responses that could be elicited within a minute was ≤5. Responsiveness recovered within several minutes. While the responsiveness to stimulation of a given nematocyte was still reduced, stimulation of another nematocyte could induce a maximal response in the recorded cell (Fig. 3A), similar to that described above for sensory hair cell stimulation. However, when the probe was lecithin-coated and stimulus repetition rates were near or above 1 Hz, consecutive response amplitudes usually increased and latencies decreased. This increase of amplitudes usually culminated and coincided with the discharge of the stimulated cell (Fig. 2C,D). The spatial distance between the stimulated and the responding nematocyte, measured as the divergence angle φ (Fig. 1), had no detectable influence on the amplitude or latency of L-potentials (Fig. 3D).

(3) Pulling at the everted tubule (thread) of a discharged nematocyte induced L-potentials with a latency of about 100 ms and reproducible amplitude and time course at repetition rates of stimuli below 1 Hz. The probe was hooked behind one of the stylets of the tubule and displaced the tubule by about 1 µm. We assume that in this setting a sensory rootlet cell close to the discharged nematocyte was stimulated (Holtmann and Thurm, 2001b) instead of the injured cell itself.

T-potentials

T-potentials appeared as discrete 'transient' voltage changes, more uniform in time course than L-potentials (Fig. 4) and somewhat reminiscent of action potentials. Compared to L-potentials, their kinetics was faster, yet variable (Fig. 4C,D; supplementary material Table S1). Overlap of T-potentials caused only little summation (3 in Fig. 4C). T-potentials often occurred repetitively in a regular pattern of up to 3 s^{-1}. At frequencies of ≥1 s^{-1} amplitudes decreased with the number of potentials (Fig. 4F,G). The maximal amplitude was 40 mV in *Stauridiosarsia* and 55 mV in *Coryne*.

In a subset of nematocytes (8% in *Stauridiosarsia*, 100% in *Coryne* and *Dipurena*) the depolarization was followed by a hyperpolarizing phase (maximal amplitude –3 mV in *Stauridiosarsia*, –11 mV in *Coryne*; Fig. 4D,E). A steep repolarization preceded the hyperpolarization. Thus, the duration of the depolarizing phase varied considerably, corresponding to the amplitude of the hyperpolarizing phase and yielding a duration at half amplitude between 5 and 32 ms in *Stauridiosarsia*. The amplitude of the actual hyperpolarization decreased with frequency (Fig. 4H) and number of repetitions (not shown) and was independent of the depolarizing phase (Fig. 4D 1).

T-potentials were generally accompanied by contractions of the epitheliomuscular cells of the tentacular shaft. Besides occurring spontaneously, i.e. without intended stimulation, T-potential and contraction were induced by the following mechanical stimulations: (i) a movement of a few micrometres of the probe against the tentacular shaft ('impact'; Fig. 4A); (ii) a forced bending of the shaft, (iii) contact of the glass probe with the cut surface of the shaft, (iv) combined mechanical and contact-chemical stimulation of a cnidocil (Fig. 3A and Fig. 5A), (v) a discharge of a nematocyte (Fig. 2D and Fig. 4F), (vi) pulling at the everted tubule (thread) of a discharged nematocyte (Fig. 4E 2 and Fig. 7C). In this case it was most obvious that the contractions occurred asymmetrically, leading to a bend of the tentacular shaft towards the site of stimulation.

Single T-potentials induced by small impacts at the shaft (Fig. 4A) occurred with latencies of 30–100 ms (*Stauridiosarsia*). The contractile twitch of the shaft was delayed by an additional 20–40 ms (*Coryne*).

Signals are not propagated *via* the environmental space

The observed inter-cellular communication could be mediated by a chemical or mechanical effect emitted by the stimulated cell into the surrounding sea water, which in turn may trigger the electrical events observed in other nematocytes. In particular, it is conceivable that the discharge of a nematocyte emits some stimulatory substance or pressure wave. To test this hypothesis, we stimulated nematocytes in one tentacle, inducing discharge (*N*=6), while recording from nematocytes in a second, separate tentacle about 80 µm apart. No response occurred under these conditions, whereas responses could be evoked when two cells a similar distance apart were part of the same tentacle.

Role of electrical coupling?

The contribution of electrical coupling of cells *via* gap junctions was tested by applying octanol (1 mmol l^{-1}; DMSO added, see Methods). Octanol did not change the sensitivity of nematocytes to discharge at adequate chemo-mechanical or local electrical stimulation. In the presence of octanol, L-potentials occurred in nematocytes as usual when a distant nematocyte discharged (*N*=4) or was stimulated at sub-threshold strength. However, T-responses were completely absent in the presence of octanol, even when the stimulated nematocyte discharged. In the absence of octanol, in contrast, 90% of all distant discharge events were associated with a series of T-potentials (Fig. 4F). Moreover, no spontaneous T-potentials occurred in the presence of octanol.

Voltage dependence and reversal potentials

In order to study the voltage dependence of the conductances underlying T- and L-responses, nematocytes of *Stauridiosarsia* were voltage-clamped and responses were evoked by mechanical stimulation as shown in Fig. 2C,D and Fig. 3A. At clamped membrane voltages near the resting potential of nematocytes (–50 to –70 mV),

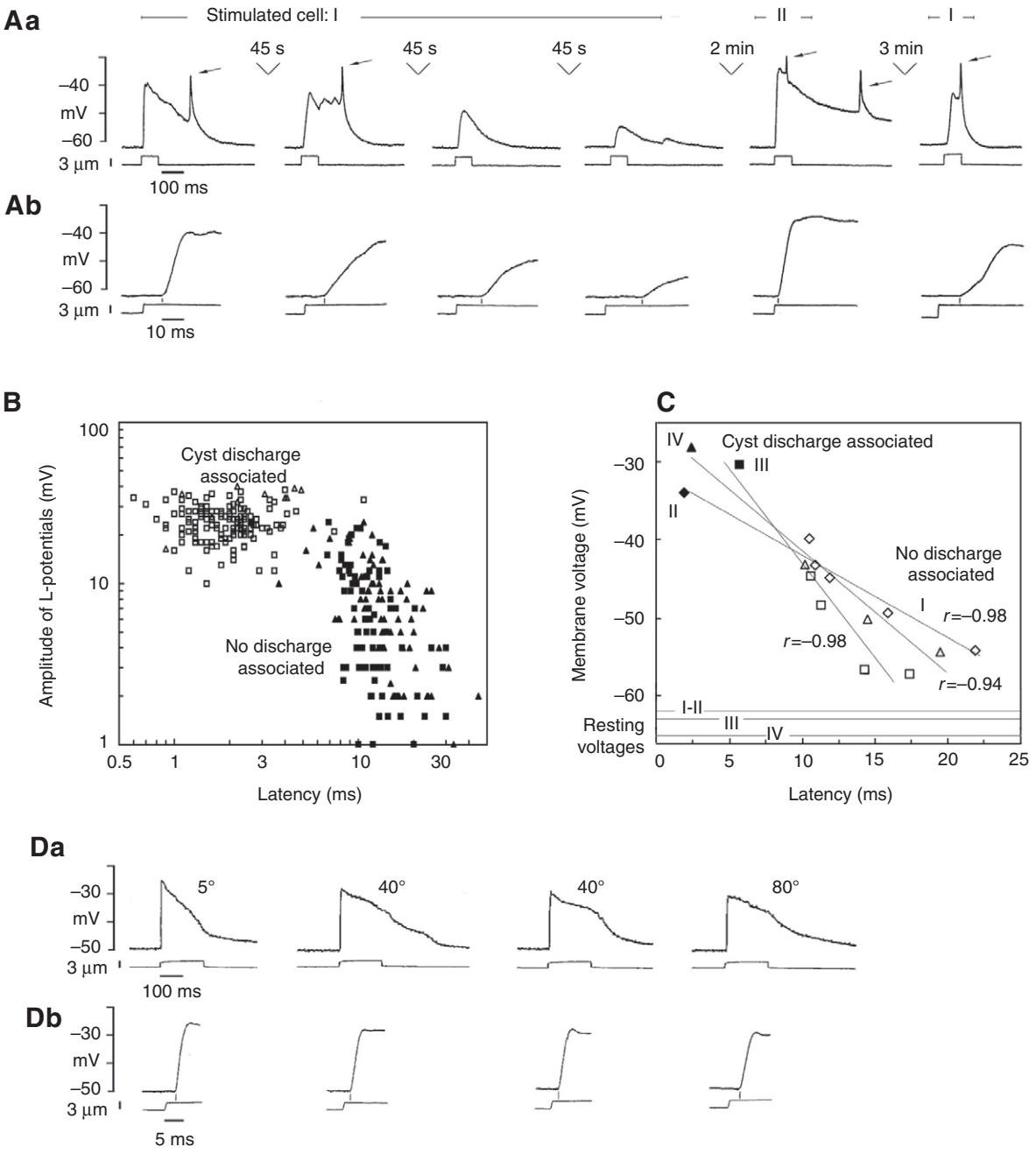

Fig. 3. (A) Series of L-potentials induced in the same nematocyte by chemo-mechanically stimulating the cnidocil apparatus of a distant nematocyte (saturating amplitude). Time intervals between records as indicated. The stimuli 1–4 and 6 (left to right) stimulated the same cell (cell I) but stimulus 5 deflected the cnidocil apparatus of another nematocyte (stimulated cell II) and induced the discharge of its cyst. Thin arrows indicate T-potentials. The initial phases of the responses and stimuli in Aa are shown on an enlarged time scale in Ab. Note the trend in the amplitudes of the L-potentials and the correlated changes in their latencies. (B) Amplitudes of L-potentials plotted against the latencies of the same responses; both axes with logarithmic scales. Values of L-potentials that occurred associated with discharge of the cyst of the stimulated cell are marked by open symbols (N=136), those that occurred without cyst-discharge (N=164) are marked by filled symbols. Open and filled triangles represent potentials induced by purely mechanical stimuli; open and filled squares represent those induced by combined chemo-mechanical stimuli. Values are from 222 stimulated cells. (C) Peak voltages of L-potentials of three recorded cells (series as in A), plotted against the latency of the same responses. Each recorded cell is represented by one symbol (square, triangle or diamond), each pair of a stimulated and a recorded cell by a roman number. Data points of series I–II are from records shown in A. Filled symbols represent responses accompanied by the discharge of the cyst of the stimulated cell; open symbols represent responses not accompanied by discharge. Resting voltages of the recorded cells as indicated. Values of r are correlation coefficients; lines indicate linear regression. Differences between absolute peak voltages of discharge associated L-potentials are smaller than the amplitudes. (D) L-potentials induced in the same nematocyte (*Stauridiosarsia*) by chemo-mechanical stimulation of other nematocytes that diverged from the recorded cell by the angles φ, given above the records. Each of these responses was associated with cyst discharge of the stimulated cell. The rising phase of each response and stimulus shown in Da is shown at higher time resolution in Db.

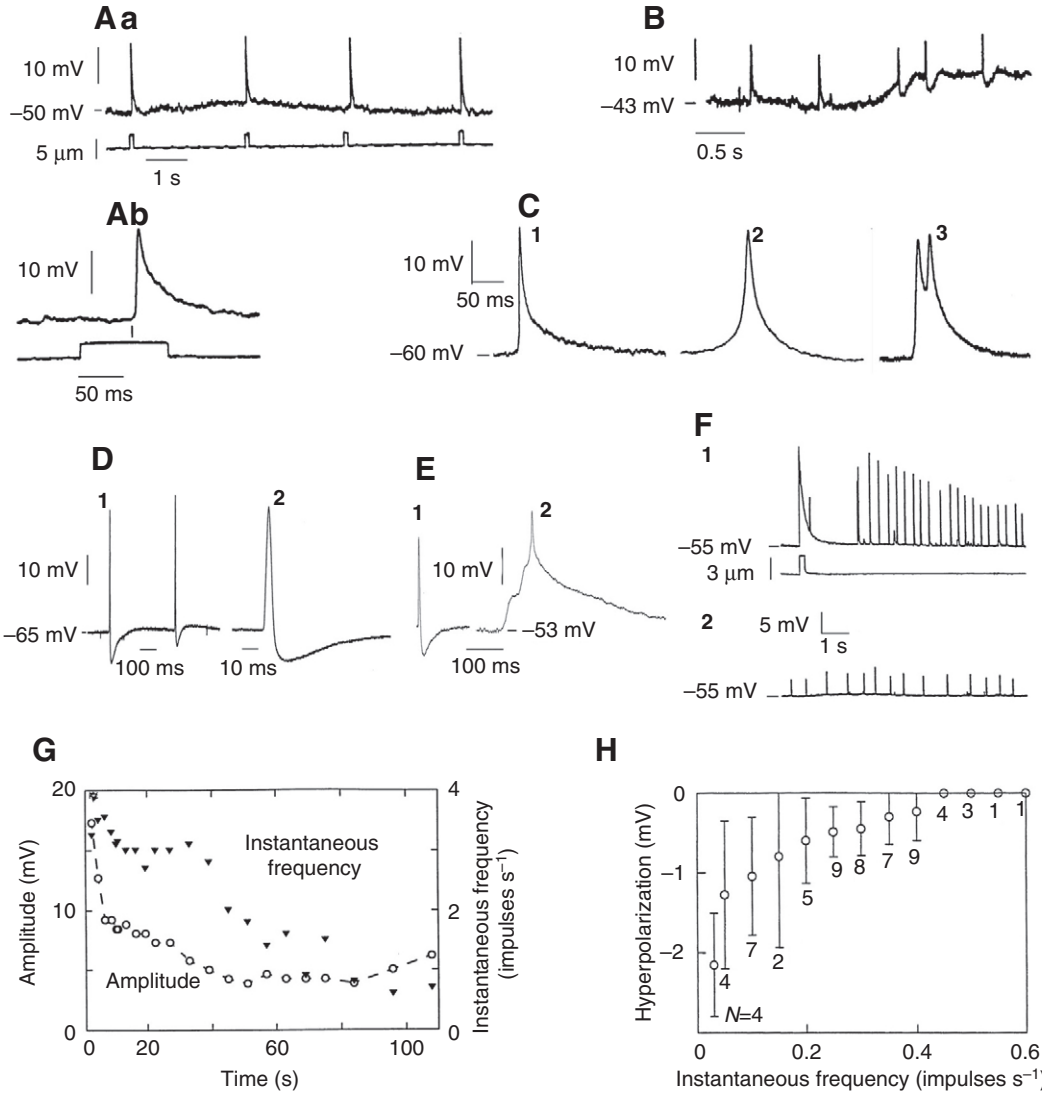

Fig. 4. T-potentials in nematocytes of *Stauridiosarsia* (A–C,F–H), *Coryne* (D) and *Dipurena* (E). Membrane voltage (upper traces) and probe excursion (lower traces) as in Fig. 2. (A) T-potentials induced by contacts of the probe with an area of the tentacle distant from nematocytes; the first response of Aa is enlarged in Ab. (B) A hyper-/re-polarizing component was observable at depolarizing membrane voltage. (C–E) Representative waveforms of T-potentials recorded from nematocytes of *Stauridiosarsia* (C), *Coryne* (D), and *Dipurena* (E). E 2 shows the superposition of L- and T-potentials, typically occurring in *Dipurena* upon mechanical stimulation of nematocytes or, here, pulling at the stinging thread of a discharged nematocyst. (F 1,2) Series of T-potentials following an L-potential that was induced by a discharge-triggering stimulation of a distant nematocyte; F 2 is a section of the same 'tail' of T-potentials, recorded 1 min after F 1. (G) Time course of amplitude and instantaneous frequency of the series of T-potentials illustrated in F. (H) Mean (± s.d.) of the hyperpolarizing component of T-potentials as a function of the instantaneous frequency of preceding T-potentials (intervals averaging 20 s; *N*=number of trials).

we recorded current responses with time courses similar to those of L- and T-potentials (Fig. 5A,B and Fig. 5C, respectively).

For a closer examination of T-responses, the tentacular shaft was stimulated repetitively. Current responses evoked at potentials between –70 and +130 mV (Fig. 5D,E) showed a near-linear dependence on membrane voltage (Fig. 5E), with a reversal potential between –5 mV and +29 mV (mean=+11±14 mV, *N*=4). At resting potential (–50 to –60 mV) the peak current was up to 1.5 nA. According to these results, the conductance that produces depolarizing T-type responses is voltage insensitive and amounts to about 20 nS.

At reduced negative membrane voltages, the initial inward current was often followed by an outward current. This delayed current occurred even in cells lacking a hyperpolarizing phase at unclamped resting potential (Fig. 5D, see also Fig. 4B). Its voltage dependence indicates a negative reversal potential down to –70 mV in *Coryne* (c.f. Fig. 4D). Under voltage clamp, the rise of the delayed outward current curtails the decay of the initial inward current (at –10 mV; e.g. Fig. 5D), indicating that the onset of this hyperpolarizing component occurs during the depolarizing current.

Since the spike-like appearance of the T-potentials initially suggested some relation to action potentials, we further characterized the conductances underlying regenerative spiking in nematocytes (Brinkmann et al., 1996). Action potentials, in contrast to T-potentials, could be elicited in nematocytes by depolarizing the cell to above –15 mV (threshold in *Stauridiosarsia*: –7.7±2.6 mV, *N*=30; Fig. 6A–C). In voltage clamp, a corresponding voltage-dependent conductance was activated above –10 mV (Fig. 6D,E). Additionally, in many cells a non-inactivating voltage-sensitive conductance was activated at about –40 mV (Fig. 6C). The resulting regenerative voltage step could boost a depolarization to elicit an action potential. Each suprathreshold current injection elicited only one action potential, independent of the duration of depolarization.

We conclude that despite their impulse-like time course, T-potentials are non-regenerative and clearly discernable from action potentials of the nematocyte.

Ionic dependence of L- and T-potentials

Dependence on sodium

Substitution of sodium by choline reversibly abolished T-potentials in *Stauridiosarsia* within about 4 min; recovery after return to ASW also required about 4 min (Fig. 7A). Substitution of sodium by choline also blocked action potentials of nematocytes (not shown). Na^+ dependence of L-potentials was not systematically tested, as the nematocyte discharge that induces L-potentials also required Na^+ (data not shown). However, L-potentials seem to have a different

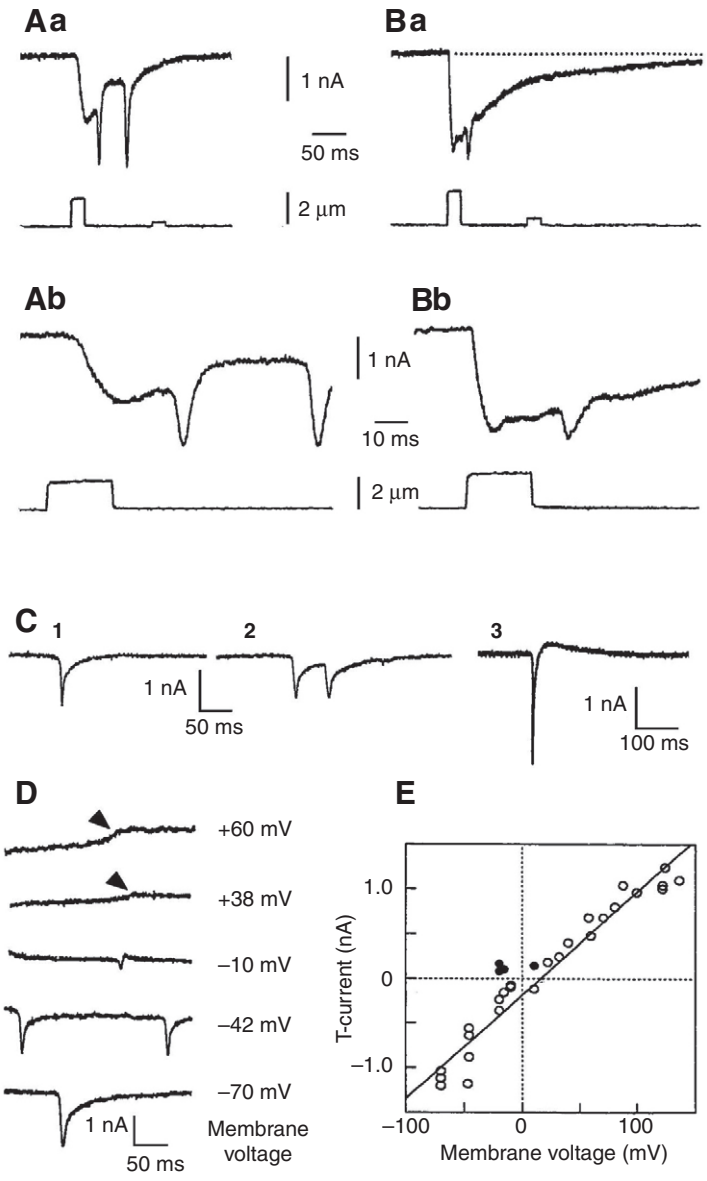

Fig. 5. Membrane currents of L- and T-responses of nematocytes. (Aa, Ba) Two L-responses of the same nematocyte (voltage-clamped near the resting potential) induced by deflections of the same cnidocil apparatus of a distant nematocyte with a time interval of 0.6 s. The L-response in B was associated with cyst discharge of the stimulated cell. T-events occurred superimposed on the L-responses. Lower traces: probe excursions (the small second excursions did not reach the cnidocil). (Ab, Bb) Higher time resolution of the initial phases of the responses. Note the earlier and steeper start of the L-response in B. (C) Membrane currents of T-events recorded when the membrane voltage was clamped at –70 mV. (D) T-currents at various clamped membrane voltages; voltages indicated next to the traces. Arrowheads indicate steps of outward current at reversed membrane voltages. Note sign reversal of the current at clamped –10 mV. (E) Amplitudes of T-currents as a function of clamped membrane voltage. Filled circles indicate the second outward current component of two-phase events. The straight line indicates a linear fit to the data. All records from *Stauridiosarsia*.

Na^+ dependence than T-potentials, as L-potentials could be induced without amplitude change only 35 s after sodium re-addition (following 4 min of sodium removal), while T-potentials were still abolished.

Dependence on calcium

In 'Ca^{2+}-free' sea water (ASW without Ca^{2+} added) T-potentials were reversibly reduced to nearly 0 mV within 1 min (Fig. 7B). By contrast, action potentials remained unchanged by a reduction of $[Ca^{2+}]$ to as low as 0.1 mmol l^{-1} (not shown). L-potentials have not been tested in Ca^{2+}-free seawater, since removal of Ca^{2+} impairs their stimulatory input, i.e. the stability of hair bundles (Brinkmann et al., 1996). At a tenfold reduction of the Ca^{2+} concentration to 0.9 mmol l^{-1} L-potentials remained constant in amplitude while the amplitude of T-potentials was reduced to about 5 mV.

Dependence on Mg^{2+}/Ca^{2+} ratio

When we reduced Ca^{2+} concentration as in the previous experiment (1 mmol l^{-1}) but increased Mg^{2+} concentration twofold (96 mmol l^{-1}; i.e. Mg^{2+}/Ca^{2+} ratio increased 18-fold) both L- and T-responses were completely abolished within 5 min (Fig. 7C). Restitution of normal ASW reversed the effect within 3–5 min. The reverse, a reduction of $[Mg^{2+}]$ to about 10% (5 mmol l^{-1}) with an unchanged $[Ca^{2+}]$, changed the spontaneous occurrence of T-potentials within 1 min to irregularly long-lasting (up to >1 s) and partially multi-phasic potentials (Fig. 7D).

Involvement of neurotransmitter receptors

We studied the effects of modulators of synaptic transmission in *Dipurena*. The responses of a given nematocyte were highly reproducible when a distant nematocyte was stimulated repetitively at intervals of approximately 1 min, using purely mechanical stimuli of constant strength that did not induce discharge. Each agent was tested on at least five recorded cells of at least two polyps.

Superfusion with 50 mmol l^{-1} sodium glutamate in ASW caused a reversible tonic depolarization of the nematocytes of 9±3 mV within 5 min (Fig. 8A). Simultaneously, the amplitudes of superimposed L- and T-potentials decreased from 42±5 mV to 32±5 mV (Fig. 8Ab), i.e. the absolute peak voltage remained about constant.

The glutamate kainate antagonist NS102 (5 µmol l^{-1}; 0.025% DMSO added, see Materials and methods) reduced the amplitudes of the superimposed L- and T-potentials of *Dipurena* reversibly to less than 2 mV within about 30 min (Fig. 8B). A similar result was obtained for pure L-potentials in *Coryne*. The superimposed L- and T-components of *Dipurena* reduced their amplitudes synchronously and continuously, suggesting that the disappearance of T-potentials is not a consequence of the blockage of L-potentials but that the antagonist affects both types of potentials simultaneously.

The cholinergic agonists acetylcholine (0.1–5 mmol l^{-1}) and carbachol (0.1 pmol l^{-1} to 1 mmol l^{-1}) had no detectable influence on L- and T-potentials. Acetylcholine (5 mmol l^{-1}), however, reversibly paralyzed the contractility of the whole superfused polyps within 5–10 s. Carbachol efficiently sensitized nematocytes, as already described (Sieger and Thurm, 1997).

The cholinergic antagonist mecamylamine blocked the hyperpolarizing component of T-potentials reversibly at a concentration of 10 µmol l^{-1} within 5 min (Fig. 8C). The opposite effect was exerted by physostigmine, a blocker of choline esterase: 100 µmol l^{-1} physostigmine doubled the hyperpolarizing amplitude and increased its duration at half amplitude from 210±63 ms to 418±85 ms (N=5; Fig. 8D).

Reserpine, applied in order to test for an involvement of catecholamines or serotonin, had no noticeable effect on L- and T-potentials in concentrations of 1–100 µmol l^{-1}.

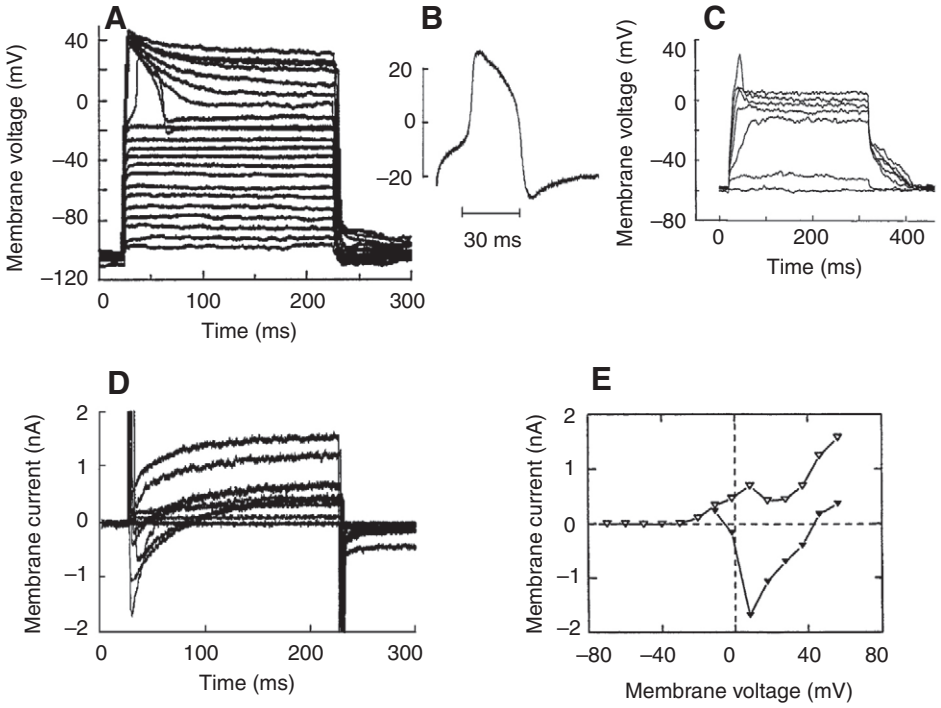

Fig. 6. Voltage sensitivity of nematocytes in the absence of chemical sensitization. (A) Voltage responses of a nematocyte from *Stauridiosarsia* to depolarizing current steps, increased in increments of 0.25 nA, starting from –100 mV. At depolarizations above –10 mV a regenerative action potential is elicited. (B) Typical action potential at a threshold of –8 mV, induced by current injection. (C) Voltage responses of a nematocyte from *Dipurena* to depolarizing current steps, increased in increments of 0.5 nA, starting from resting voltage. At about –40 mV a regenerative, persistent depolarization is triggered, while an action potential occurs at a threshold close to 0 mV. (D) Membrane currents from a *Stauridiosarsia* nematocyte recorded in discontinuous voltage-clamp mode in response to voltage steps in increments of 10 mV, starting from –70 mV (data are shown with linear leak currents subtracted). (E) Membrane currents from D as a function of membrane potential: steady-state currents (open symbols) are compared to transient values (filled symbols). Transient inward currents activate at about –10 mV, matching the action potentials threshold.

Electrical stimulation of presynaptic nematocytes

In order to directly test a relationship between pre- and postsynaptic electrical events of communicating nematocytes, we bypassed mechanoelectrical transduction by directly applying square pulses of voltage to single nematocytes, using a transepithelial configuration of electrodes (see Materials and methods). As described above for mechanical stimulation, the membrane voltage of distant nematocytes was recorded simultaneously.

Basolaterally depolarizing (anodic) voltage pulses of 100–200 mV at 20–40 ms duration induced L-potentials in distant nematocytes with characteristics as shown before (Fig. 2E). Similar to the largest L-potentials, the responding cell depolarized up to about –25 mV when the stimulated cell discharged (eight of 12 stimulated cells). Responses that were not associated with a discharge of the stimulated cell had variable sub-maximal amplitudes (Fig. 2E).

Apically depolarizing (cathodic) pulses elicited discharge of the stimulated nematocyte at considerably smaller amplitude: –25 to –95 mV [comparable to results obtained with Hydra (Gitter and Thurm, 1996)]. In the recorded nematocytes (N=6) these discharges were associated with a large L-potential of short latency (<10 ms) and by superimposed T-potentials, as described above for discharges elicited mechanically (Fig. 2F; c.f. Fig. 2D and Fig. 3A, cell II). When a cathodic pulse did not elicit a discharge it did not induce an L- or T-potential; i.e. these basolaterally hyperpolarizing impulses did not induce sub-maximal, graded L-potentials, in contrast to basolaterally depolarizing impulses.

DISCUSSION

Cellular mechanisms underlying the generation of L- and T-potentials

Our intracellular recording from nematocytes revealed that mechanical stimulation of single nematocytes and hair cells is reflected in distant nematocytes as delayed voltage signals that are distinct from receptor potentials (Brinkmann et al., 1996). We classify these signals according to their different stimulus-dependent properties. (1) L-potentials: these are characterized by a graded amplitude between a few mV and 40 mV and of variable duration. These parameters correlate to some degree with parameters of the stimulus, however, less strictly than found for receptor potentials (Brinkmann et al., 1996). (2) T-potentials: the time course and occurrence is comparable with those of action potentials as they have stereotyped impulse-like waveforms with a variable number and frequency of repetitions.

Are T-potentials actually action potentials as Price and Anderson (Price and Anderson, 2006) proposed for T-potential-like responses of *Cladonema*, a capitate hydroid closely related to the species examined in this study? Their ‘Class I’ and ‘Class II’ potentials were induced in nematocytes by water-borne chemosensory stimulation of the isolated tentacle. Two of our findings show that the ion channels which generate T-potentials are electrically non-excitable: (1) T-potentials cannot be triggered by depolarization of the recorded nematocyte; (2) the current–voltage relationship of T-potentials is linear. Genuine action potentials, by contrast, can indeed be triggered electrically in nematocytes as demonstrated in Fig. 5 (see also Brinkmann et al., 1996; Anderson and McKay, 1987). However, their threshold is remarkably high (–10 mV) and is usually not even reached by the peaks of T-potentials. Moreover, T-potentials are different in their Ca^{2+} dependence and time course from the action potentials of the same cells. These findings unequivocally reveal that T-potentials are not action potentials.

Are T- and/or L-potentials conducted electrotonically from a separate cellular source into the observed nematocyte, e.g. *via* gap junctions? Since Price and Anderson (Price and Anderson, 2006) proposed that nematocytes in *Cladonema* are electrically coupled to one another, implying that ‘Class I and II potentials’ were conducted from cell to cell, we carefully considered this possibility. However, several lines of evidence converge to the conclusion that intact nematocytes are not electrically coupled.

(1) Detailed ultrastructural studies in *Coryne* did not reveal gap junctions in nematocytes, but between supporting cells, which separate nematocytes from each other (Holtmann and Thurm, 2001b). As a caveat, it cannot be excluded that cell couplings of

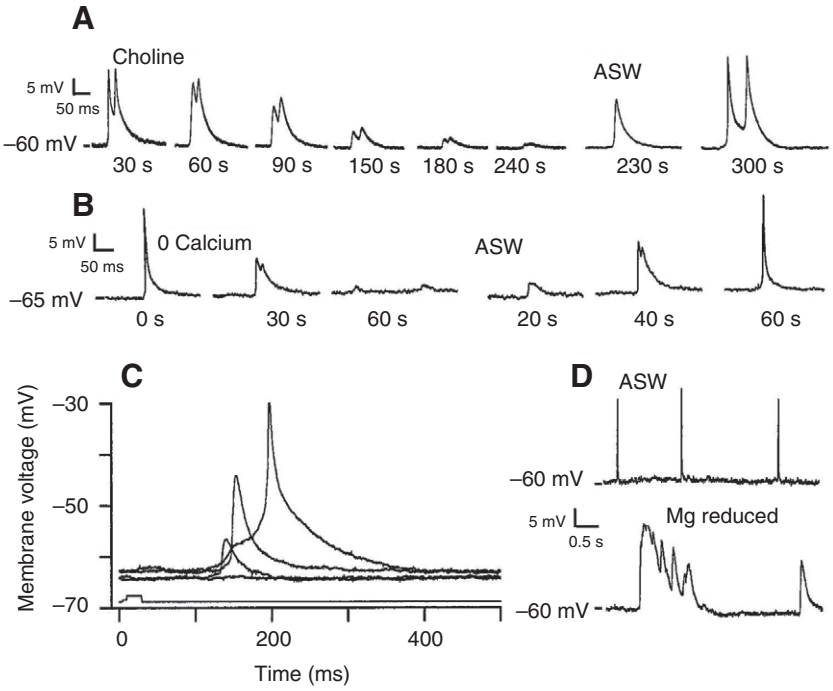

Fig. 7. Ionic dependence of T- and L-potentials. (A) T-potentials during substitution of sodium in ASW by choline and after restitution of ASW. Data below the traces indicate time after exchange of solution. (B) T-potentials during superfusion with '0 Ca^{2+}-ASW' (i.e. no Ca^{2+} added) and subsequent exchange with regular ASW. Data below records as in A. (C) L- and superimposed T-potentials during superfusion with ASW containing 1 mmol l^{-1} Ca^{2+} and double the Mg^{2+} concentration (96 mmol l^{-1} Mg^{2+}); highest response amplitude recorded immediately before switching to the test medium; progressively reduced amplitudes recorded at 3, 4 and 5 min of superfusion by the test medium. Records from *Dipurena*. Lower trace: excursion of the stimulus probe pulling at a stinging thread of a discharged nematocyst. (D) Effect of reduced Mg^{2+} concentration on T-potentials: upper trace before, lower trace 1 min after reduction of [Mg^{2+}] to 10% (5 mmol l^{-1}) in ASW. All records except those in C from *Stauridiosarsia*.

minute size, as described by Germain and Anctil (Germain and Anctil, 1996), might have been overlooked in nematocytes.

(2) Functional evidence supports the lack of gap junctions in nematocytes. Thus, the gap-junction-permeable stain Lucifer Yellow injected into nematocytes remained restricted to these cells [experiments with *Physalia* (Purcell and Anderson, 1995); *Stauridiosarsia* (Brinkmann et al., 1996); *Hydra* (Lawonn, 1999)]. However, when the dye was injected into an epitheliomuscular cell, it spread into neighbouring epitheliomuscular cells, but not into nematocytes [experiments in *Hydra* (Lawonn, 1999)]. Octanol, known to block gap junctions of hydrozoans as well as of anthozoans (Dunlap et al., 1987; Mire et al., 2000), prevented the spread of Lucifer Yellow between epitheliomuscular cells (Lawonn, 1999). It should be mentioned that one study (Price and Anderson, 2006) observed spreading of Lucifer Yellow from an injected to neighbouring nematocytes and to other unidentified cells 'with time' and after prolonged injection of stain (5–20 min, unspecified current strength). It seems possible that this spreading was due to deterioration of the impaled cell. It was not blocked by heptanol and octanol. However, electrical coupling of cells can exist even if Lucifer Yellow is not able to permeate (Murphey et al., 1983; Shibayama et al., 2005).

(3) Electrical tests of cell coupling using current injection have led to contradictory conclusions, although the studied nematocytes showed similar chemosensory responses [studying *Physalia*: no coupling between nematocytes (Purcell and Anderson, 1995); studying *Cladonema*: coupling between nematocytes (Price and Anderson, 2006)]. These measurements may have produced ambiguous results because the reference electrode for injected current was located outside the epithelial tissue. Thus this current could lead to voltage drops across cells surrounding the injected cell even if these cells were not directly coupled to the cell receiving the current injection (c.f. Fig. 2E,F).

(4) We avoided this problem by using the mechanoreceptor potential of nematocytes as a physiological tracer for electrical coupling. Receptor potentials are clearly different from L-potentials in their latency and kinetics (Brinkmann et al., 1996; Thurm et al., 1998a; Thurm et al., 1998b; Thurm et al., 2004). In more than 50 recorded nematocytes the stimulation of neighbouring or distant nematocytes never led to the occurrence of any attenuated receptor potential but was exclusively reflected by L-potentials. Accordingly, nematocytes were neither directly nor indirectly electrically coupled with each other. The same conclusion holds true for nematocytes from *Cladonema*: large L-potential-like potentials ('Class III') induced by adequate chemical stimuli were not reflected in neighbouring nematocytes (Price and Anderson, 2006), arguing against any ohmic coupling between these cells. In principle, one cannot exclude artificial decoupling of a nematocyte induced by penetration of the microelectrode. However, all impaled and successfully observed cells in our study showed T-potentials in the absence of electrical coupling of receptor potentials, arguing against an electrotonic origin of T-potentials. This conclusion cannot be disproved either by the synchronicity of T-potential-like potentials in neighbouring nematocytes as observed in *Cladonema* and *Physalia* (Purcell and Anderson, 1995; Price and Anderson, 2006) or by the block of T-potentials under Octanol that we observed. Both findings will be discussed below as being due to the presynaptic signal source.

(5) For T-potentials, the reversal potential is particularly revealing since it is consistent with the non-specific cationic conductance characteristic of conventional EPSPs. This provides direct evidence that the electrical source of these potentials is located within the recorded nematocyte. [To depolarize a cell to an EPSP-reversal potential needs a continuous current flow. If this current crosses the resistance of a gap junction in series with the postsynaptic cell it produces a voltage across this resistance. The measured (apparent) reversal potential must deviate from the true reversal potential that would be measured in the postsynaptic cell by this voltage drop (e.g. see Johnston and Wu, 1995). The amount of deviation depends on the coupling coefficient. Even a low resistance coupling, with coupling coefficient 0.5, would increase the difference between resting and true reversal potential by 100%. The amplitude of regular T-potentials argues against such an error in the measured reversal potential.]

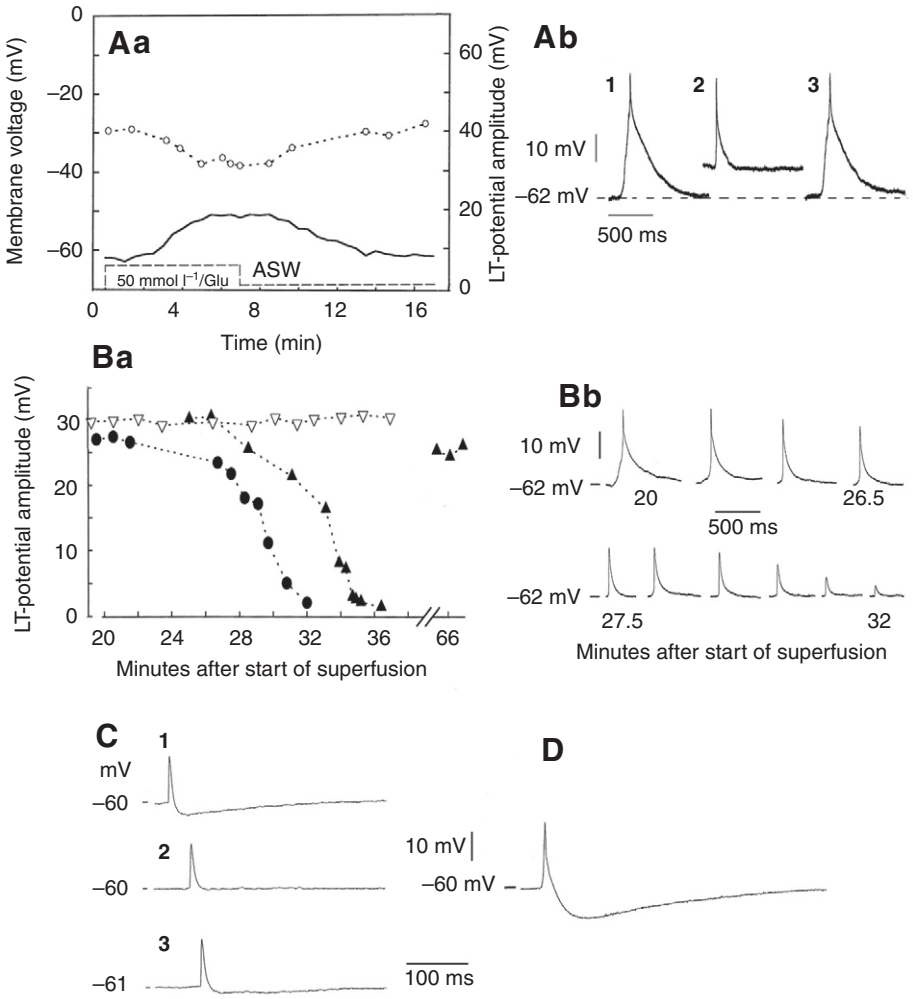

Fig. 8. Effects of transmitter agonists and antagonists on L- and T-potentials. All recordings from *Dipurena*. (Aa) Effect of glutamate (50 mmol l^{-1} sodium glutamate) on resting potential (continuous line) and amplitude of superimposed LT-potentials (circles and dotted line). Superfusion with glutamate-ASW as indicated. (Ab) Records of superimposed LT-potentials: (1) before, (2) during, (3) after the application of glutamate. (Ba) Effect of NS102 (5 μmol l^{-1}, with 0.025% DMSO), a blocker of kainate glutamate receptors, on the amplitude of superimposed LT-potentials of two nematocytes (filled circles and triangles). A third cell (control; open triangles) exposed to 0.025% DMSO only in ASW. Re-impaling the second cell (filled triangles) after wash-out of the blocker tested the reversibility of its action. (Bb) LT-potentials of the first cell recorded 20–32 min (data given below the records) after start of superfusion with NS102; recorded at the times indicated in Ba. The resting potential remained constant at –62 mV. (C) T-potentials recorded before (1), 5 min after the start (2), and 5 min after the end (3) of superfusion with mecamylamine (10 μmol l^{-1}). (D) T-potential recorded during superfusion with physostigmine (100 μmol l^{-1}). Prior to application of physostigmine, the amplitude of the hyperpolarizing component was 5 mV, analogue to C 1.

Altogether, our findings indicate that T- or L-potentials do not enter nematocytes by passive propagation *via* gap junctions. Thus, the electrical sources of L- and T-potentials must be located in the recorded nematocyte itself, suggesting a postsynaptic mechanism. In fact, we found features of chemical synapses. L- and T-potentials were blocked by an increase in [Mg^{2+}] at reduced Ca^{2+}-concentration, typical for an exocytotic mechanism (Katz and Miledi, 1967). Furthermore, L- and T-potentials were abolished by antagonists of the neurotransmitters glutamate and acetylcholine, respectively, while glutamate depolarized the cell, and blocking of acetylcholine-degradation increased hyperpolarizing responses. Long delays of all these actions (5–30 min) indicate low accessibility of the site of action and suggest considerable difference between applied and effective concentrations. Electron microscopy revealed afferent and efferent synaptic structures located basally at the nematocytes and separated from the surface medium by septate junctions, known as diffusion barriers (Holtmann and Thurm, 2001a; Holtmann and Thurm, 2001b). Histochemical identification of glutamate receptors at nematocytes has been reported (Kass-Simon and Scappaticci, 2004; Kass-Simon and Pierobon, 2007).

From this set of results we conclude that both, L- and T-potentials are postsynaptic potentials (PSPs), probably induced by glutamate; both are excitatory (EPSP), with the exception of the hyperpolarizing second component of T-potentials. According to the nicotinic pharmacology and delayed time course, this latter component is probably a separate, though tightly EPSP-coupled, synaptic event. Its hyperpolarization caused by a negative reversal potential characterizes it as an inhibitory PSP (IPSP). Purely hyperpolarizing T-PSP-like potentials that occur independently of a depolarizing component have been found previously in epitheliomuscular cells of *Hydra* (Lawonn, 1999).

The magnitude of the T-IPSP phase differed between different species and individual cells and thus contributed to the considerable variability of the time course and duration of T-potentials, since the inhibitory component curtailed the excitatory to varying degrees, depending on their amplitude ratio and phase relation. When T-potentials occurred repetitively, the amplitudes of T-EPSPs and T-IPSPs decreased independently of each other with the number and frequency of repetitions (c.f. Fig. 4G and Fig. 3H). These reductions may be interpreted as synaptic depression at two independent synaptic sites that are driven from a common source of excitation. The same processes are likely to explain the differences between ‘Class I’ and ‘Class II’ potentials and their variability and transitions, which Price and Anderson (Price and Anderson, 2006) found to be induced by chemosensory stimulation in the nematocytes of *Cladonema*.

Neuronal connectivity underlying the generation of synaptic signals in nematocytes

L- and T-potentials largely differ in their induction, time course and susceptibility to the gap-junction blocker octanol. These differences

provide important insights into their presynaptic input, electrical signalling and neuronal connectivity.

L-potentials were induced by mechanical stimulation of single sensory hair cells and mechanical or electrical stimulation of other nematocytes. Hair cells are in somato-somatic synaptic contact with nematocytes and nematocytes are in somato-neuritic contact with other nematocytes (Holtmann and Thurm, 2001a). Taken together, our results and previous ultrastructural findings suggest that L-potentials should arise from monosynaptic transmission and that presynaptic receptor potentials as well as action potentials (Brinkmann et al., 1996) can induce postsynaptic L-potentials. However, with monosynaptic transmission, why do L-potentials show such variable amplitudes and latencies, in particular the conspicuous differences between those L-responses associated with discharge of the stimulated cyst and those not discharge-associated (Fig. 3B,C)? Considering the putative presynaptic potentials sheds some light on the mechanisms underlying these differences. The discharge of a cyst is associated with an action potential triggered by a receptor potential or by injected current (Brinkmann, 1994; Brinkmann et al., 1996). The presynaptic event of discharge-associated L-potentials is a 'standardized' signal with an amplitude of about 80 mV, consistent with the relatively uniform amplitudes of these L-potentials of 25±6 mV (up to 44 mV) and with the uniform latencies of 2.1±1.2 ms. However, L-potentials that were not discharge-accompanied reached amplitudes of 24 mV at most, despite being recorded from the same pairs of nematocytes and induced by equally saturating mechanical stimuli as the discharge-associated L-potentials. Receptor potentials, measured under these conditions, had amplitudes of 40–50 mV and mostly did not elicit an action potential (Brinkmann et al., 1996). This indicates that the postsynaptic voltage signal is a function of the presynaptic signal amplitude, i.e. the synapse generating L-potentials works in a graded manner.

However, in the absence of a discharge, L-EPSPs showed a correlated variation in amplitude and in latency. Typically, such variation occurred as a gradual decline of L-potential amplitude with concomitant increase in latency upon repeated mechanical stimulation of the presynaptic cell of a given pair of nematocytes. This finding suggests that the synaptic process that generates L-potentials is subject to strong synaptic depression. Several lines of evidence suggest that this alteration targets synaptic mechanisms in the presynaptic, but not the postsynaptic cell. First, L-potentials depended on the pre-stimulus history of the stimulated cell, including repeated mechanical stimulation and chemical sensitization. Second, amplitude reduction induced by stimulation of one presynaptic cell had no impact on the size of L-potentials induced by stimulation of a different presynaptic nematocyte. Third, presynaptic receptor potentials do not show comparable adaptation in response to repeated stimulation (Brinkmann et al., 1996; Thurm et al., 2004), indicating modulation of downstream events. Finally, it is quite unlikely that the observed concomitant reduction of amplitude and increase of latencies results from a reversible and gradual change in synaptic connectivity from a monosynaptic contact to a chain of serial synapses.

In fact it has been shown that short-term plasticity, like depression, facilitation and synaptic modulation in various model synapses may involve latency increases with amplitude depression (Waldeck et al., 2000; Boudkkazi et al., 2006) and latency decreases with facilitation or positive modulation (Vyshedskiy and Lin, 1998; Vyshedskiy et al., 1998). The surprisingly large extent of use-dependent latency increase in nematocytes is associated with a unique organization of these synapses (c.f. Holtmann and Thurm, 2001a).

For comparison with delay times of established monosynaptic transmission, we only considered L-potentials that were not affected by synaptic depression, i.e. L-potentials associated with cyst-discharge. Their latencies of 2.1±1.2 ms are well within the range of delays for neuromuscular synapses of other hydrozoans, e.g. 0.9–7.0 ms in *Polyorchis* (mean 3.2 ms) (Spencer, 1982) and 0.7±0.1 ms in *Aglantha* (Kerfoot et al., 1985). It should be noted, that for meaningful comparison one has to add at least 1 ms to the motoneuronal delays since these have been measured from the peak of the presynaptic action potentials whereas L-potential latencies were measured from the onset of the mechanical stimulus [delay and rise time of the receptor potential $\geqslant$1 ms (Brinkmann et al., 1996)]. Thus, the induction of L-potentials is fully consistent with monosynaptic transmission between nematocytes.

A series of two or more nematocyte–nematocyte synapses also are conceivable, since discharge-associated L-potentials approach the amplitude of large receptor potentials; thus the L-potential itself may trigger transmission onto another nematocyte. L-potentials that result from transmission through two or three synapses sequentially may be expected to show an increased latency and a smaller amplitude. Yet, when different pairs of cells were compared, no correlation between latency and amplitude of discharge-associated L-potentials was found (Fig. 3B). However, di- or polysynaptic L-responses may instead contribute to the delayed components of large multiphasic L-potentials (Fig. 2D and Fig. 3A).

In conclusion, our data support the idea that L-potentials are predominantly transmitted by a single synaptic step and are the postsynaptic response to presynaptic receptor and action potentials of nematocytes and hair cells. This is in agreement with the ineffectiveness of the gap junction blocker octanol and previous ultrastructural data.

T-potentials, in contrast to L-potentials, were not found to have any presynaptic electrical correlate in directly stimulated and discharging nematocytes (Brinkmann, 1994; Brinkmann et al., 1996). Instead, T-potentials were evoked by mechanical stimulation at any distance from the recorded nematocyte, e.g. by minute deformations of the tentacular sphere or shaft. This suggests that the tentacular signals that ultimately induce T-potentials spread over long distances without any appreciable amplitude decay, pointing to the involvement of action potential conduction. If action potentials are the presynaptic events of T-potentials this explains the uniform amplitude and time course of T-potentials. The fact that T-potentials are mostly or always associated with contractions of epitheliomuscular cells suggests that the ectoderm is a pathway for this presynaptic conduction. T-potential-like depolarisations were indeed recorded in epitheliomuscular cells of *Hydra* (Lawonn, 1999). Gap junction-connected epitheliomusclular cells are an essential pathway of electrical signal conduction in Cnidaria (reviewed by Mackie, 2004). Their involvement explains the blockage of T-potentials by octanol. This more complex kind of signal transmission preceding T-potentials, compared with L-potentials, is well consistent with the differences between their shortest latencies (T-potentials: 30 ms; L-potentials: 0.6 ms) and the different delays of signal recovery after Na^+ removal.

Even when the site of stimulation inducing T-potentials was the tentacular sphere, epitheliomuscular cells of the tentacular shaft contracted. Thus, epithelial conduction was involved, although in the sphere non-contractile supporting cells take the place of epitheliomuscular cells. The supporting cells enclose each nematocyte and sensory cell and are interconnected *via* gap junctions like the contractile cells (Holtmann and Thurm, 2001b). As a consequence, all or many nematocytes of a tentacular sphere should

be surrounded by essentially the same flow of action potentials, leading to similar patterns of T-PSPs in all of these nematocytes. In accordance with this conclusion, Purcell and Anderson (Purcell and Anderson, 1995) and Price and Anderson (Price and Anderson, 2006) found T-potential-like EPSPs ('Class I and II potentials') that were synchronous in all recorded pairs of nematocytes within a tentacular battery of *Physalia* or a tentacle of *Cladonema*, whereas L-potential-like slow postsynaptic potentials in the same records did not exhibit coincidence (Price and Anderson, 2006), indicating that the synchrony did not result from direct electrical coupling between nematocytes.

In conclusion, our data demonstrate that T-potentials result from chemical transmission and are induced by signals conducted through the tentacle, most likely epithelial action potentials. The observation that T-potentials are composed of phase-coupled excitatory and inhibitory PSPs generated by different transmitters, points to a complex synaptic organization. More functional data are required for a mechanistic interpretation of the available ultrastructural results (Holtmann and Thurm, 2001a).

Nematocytes as sensory cells

L- and T-potentials induced by stimulation of distant nematocytes reveal that stenotele nematocytes produce afferent synaptic signals, i.e. they act as sensory cells. Evidently, the discharge of the cnidocyst is not the sole action of these cells, as often assumed, but the very last and most striking. Other types of cells, besides nematocytes, also receive afferent signals from nematocytes, as is revealed by the occurrence of T-potentials: stimulated nematocytes induce T-potentials in other nematocytes, but they do not directly produce the presynaptic potentials that elicit these T-potentials.

Probability and amplitude of L-responses were dependent on the chemical properties of the surface of the stimulation probe. Thus, nematocytes function as mechanoreceptor cells with substance-dependent mechanical sensitivity, adding a vital sensory quality to the spectrum of mechanosensation that is provided by the sensory cells (Holtmann and Thurm, 2001b). Although having no effect on the mechanoreceptor potential of nematocytes (Brinkmann et al., 1996), chemical stimuli strongly affect their exocytotic outputs, i.e. the cnidocyst discharge and presynaptic activity. Therefore, we propose that sensory bi-modality results from chemosensory modulation of the exocytotic processes [see Thurm et al. (Thurm et al., 1998b) and Appendix]. It is conceivable that the same chemosensory intracellular signalling pathway modulates both the apical cnidocyst discharge and the basolateral exocytotic release of synaptic transmitter.

Functional role of efferent signals in nematocytes

Our recordings from nematocytes revealed that these cells receive signals reflecting a considerable number of different mechanical events acting on the tentacle. Besides the mechano-chemical stimulation of other nematocytes and their cyst discharge, these stimuli are: hydrodynamic movements, touch of the tentacular surface, deformations and contractions of the tentacular shaft, and forces pulling at discharged cnidocysts. Similar responses can be induced by water-soluble chemical stimuli, as reported from other hydrozoan species (Purcell and Anderson, 1995; Price and Anderson, 2006). Both sensory modalities are reflected in the nematocytes by graded EPSPs, induced by presynaptic receptor potentials, and by more stereotyped PSPs, which we attributed to presynaptic epithelial action potentials. In contrast to *Hydra* (Thurm et al., 1998), feeding or starvation of the Corynidae did not change the behaviour of the nematocytes (D.O., M.B., T.S. and U.T., unpublished observation), which may be related to the nutritional buffer capacity of the stolonial configuration of Corynidae as opposed to non-stolonial *Hydra*.

What is the impact of L- and T-potentials on nematocyte function? So far, we can infer that synaptic depolarization adds to any receptor potential resulting from direct stimulation of the nematocyte. Synaptic potentials may thus contribute to reaching the threshold for discharge of the cnidocyst (Brinkmann et al., 1996) (c.f. Kass-Simon and Scappaticci, 2004). An opposite effect may result from the inhibitory component of T-potentials. However, T-potentials may be too brief to have substantial influence in this direct way. Instead, one may speculate that postsynaptic second messenger pathways may modulate the sensitivity or readiness of a response, comparable to the modulation exerted by contact-chemical stimulation of the cnidocil (Thurm et al., 1998b). While our study revealed the integrative signal flow to and from nematocytes, it remains a challenge for future studies to work out the cellular effects of the synaptic inputs found.

Comparative aspects of neurotransmission at nematocytes

The organization of synaptic communication of nematocytes and hair cells of hydrozoans shows an intriguing analogy to that of vertebrate hair cells. The mechanosensory cell types from both phyla are characterized by the axon-less ('secondary') type of sensory cell configuration. Graded receptor potentials are the presynaptic afferent signals in both cases, instead of action potentials as in axon-bearing sensory cells. Afferent synapses of both cell types present highly specialized, but different presynaptic structures, which may be adaptations to the specific presynaptic electrical signals. The ribbon-type afferent synapse of vertebrate hair cells uses a large number of small vesicles (Fuchs et al., 2003) whereas in nematocytes, a magno-vesicular structure comprises only one or a few unusually large vesicles (up to 1 μm in diameter) supposed to release transmitter in transient fusion and partial depletion (Neher, 1993; Holtmann and Thurm, 2001a). Both presynaptic structures are considered to be optimized for sustained transmission of the graded presynaptic signals. Similarities extend to the sensory cell's transmitters. The excitatory afference supplied by nematocytes, generating L-potentials, appears to be glutamatergic, using non-adapting kainate-like receptors. Indeed, glutamate receptors have been identified at nematocytes in *Hydra* (Kass-Simon and Scappaticci, 2004; Kass-Simon and Pierobon, 2007). Similarly, glutamate is the transmitter of the afferent synapses of vertebrate hair cells (Fuchs et al., 2003). Moreover, both nematocytes and vertebrate hair cells receive an inhibitory efference, operated by presynaptic action potentials. In nematocytes, inhibition appears to be mediated by acetylcholine *via* neuronal nicotinic-like receptors, as inhibitory T-potentials were blocked by mecamylamine. Similarly, the efferent synapses at vertebrate hair cells are cholinergic with postsynaptic nicotinic receptors (Fuchs, 1996). Their inhibitory PSPs show a biphasic behaviour somewhat reminiscent of the T-potentials characterized here, but evoked by the single transmitter which in that case activates a depolarizing Ca^{2+} influx that subsequently activates the hyperpolarizing K^+ efflux.

APPENDIX

Triggering the discharge of a cnidocyst critically depends on the time course of depolarization

We report the following results in order to draw attention to the slope of depolarization for triggering the discharge of nematocysts. The results are essential for the reproducibility of the experiments. Moreover, they may be revealing to understand the mechanism of chemical sensitization of nematocytes. The results are similarly

relevant for mechanical stimulation causing the slope of the receptor potential.

Square pulses, apically depolarizing single nematocytes at 100 mV transepithelial amplitude, triggered cnidocyst discharges with a probability of 78% (N=143), a probability much higher than that produced by purely mechanical stimulation. When, at unchanged stimulus amplitude, the steepness of apical depolarization was reduced (ramp 9 ms/90% rise, in contrast to 33 μs/90% rise of previous pulses) in order to mimic the maximal steepness of receptor potentials of nematocytes [2–4 ms/90% rise (Brinkmann et al., 1996)], the discharge probability was reduced to 10% (N=31), approaching the probability of 8% obtained by purely mechanical stimuli (N=123). Chemical sensitization of the cells by phosphatidylcholine, which increased the probability of discharge at mechanical stimulation from 8% to 67%, increased the probability of discharge for the steep electrical pulses to nearly 100%. (Phosphatidylcholine applied within the electrode capillary: see Materials and methods.)

The results reveal that the voltage-dependent process, which controls the exocytotic cyst discharge, includes a step that differentiates the time course of depolarization with a rate in the range of the steepness of receptor potentials. Consequently, changes of this rate must be crucial for changing the probability of inducing cyst discharges. As a working hypothesis we propose that reducing this crucial rate is the process of sensitization that is induced by the contact-chemoreception of the cnidocil. Earlier results suggested that the cyst discharge is initiated by voltage-controlled Ca^{2+} influx (Gitter et al., 1994; Gitter and Thurm, 1996; Thurm et al., 1998b; Nüchter et al., 2006). We suggest time-dependent inactivation of this Ca influx as a reasonable candidate for the depolarization-differentiating process that may be rate-controlled by the chemosensory modulation. We invite experiments testing this hypothesis.

This research was supported by the German Research Foundation (DFG) and the German Fonds of the Chemical Industry. We are grateful to Dr V. Schmid, Zoological Institute Basel, for the gift of *Dipurena reesi,* to Drs Elisabeth Glowatzki and Henrike Berkefeld for critical reading and linguistic improvement of the manuscript, and to two anonymous reviewers for valuable comments.

REFERENCES

Anderson, P. A. V. and McKay, M. C. (1987). The electrophysiology of cnidocytes. *J. Exp. Biol.* **133**, 215-230.
Boudkkazi, S., Carlier, E., Ankri, N., Fronzaroli, L., Caillard, O. and Debanne, D. (2006). Synaptic timing at unitary synaptic contacts between layer 5 pyramidal neurons. *FENS Abstr.* vol. 3, A151.4.
Brinkmann, A. and Petersen, K. W. (1960). On some distinguishing characters of *Dipurena reesi* Vanucci 1956 and *Cladonema radiatum* Dujardin 1843. *Publ. Stat. Napoli* **31**, 386-392.
Brinkmann, M. (1994). Das Rezeptor-Effektor-System der Nesselzellen eines Hydropolypen (Corynidae). *Inaugural-Dissertation der Naturwissenschaftlichen Fakultät der Universität Münster*, 1-115.
Brinkmann, M., Oliver, D. and Thurm, U. (1995). Interaction of mechano- and chemosensory signals within the same sensory cell. *Pflügers Arch. Eur. J. Physiol.* **429** (Suppl), R153.
Brinkmann, M., Oliver, D. and Thurm, U. (1996). Mechanoelectric transduction in nematocytes of a hydropolyp (Corynidae). *J. Comp. Physiol. A* **178**, 125-138.
Dunlap, K., Takeda, K. and Brehm, P. (1987). Activation of a calcium-dependent photoprotein by chemical signalling through gap junctions. *Nature* **325**, 60-62.
Fuchs, P. A. (1996). Synaptic transmission at vertebrate hair cells. *Curr. Opin. Neurobiol.* **13**, 514-519.
Fuchs, P. A., Glowatzki, E. and Moser, T. (2003). The afferent synapse of cochlear hair cells. *Curr. Opin. Neurobiol.* **13**, 452-458.
Germain, G. and Anctil, M. (1996). Evidence for intercellular coupling and connexin-like protein in the luminescent endoderm of *Renilla koellikeri* (Cnidaria, Anthozoa). *Biol. Bull.* **191**, 353-366.
Gitter, A. H. and Thurm, U. (1996). Rapid exocytosis of stenotele nematocysts in *Hydra vulgaris. J. Comp. Physiol. A* **178**, 117-124.
Gitter, A. H., Oliver, D. and Thurm, U. (1994). Calcium- and voltage-dependence of nematocyst discharge in *Hydra vulgaris. J. Comp. Physiol. A* **175**, 115-122.
Golz, R. (1994). The apical surface of hydrozoan nematocytes: Structural adaptations to mechanosensory and exocytotic functions. *J. Morphol.* **222**, 49-59.
Golz, R. and Thurm, U. (1991). Cytoskeleton-membrane interactions in the cnidocil complex of hydrozoan nematocytes. *Cell Tissue Res.* **263**, 573-583.
Holtmann, M. and Thurm, U. (2001a). Mono- and oligo-vesicular synapses and their connectivity in a cnidarian sensory epithelium (*Coryne tubulosa*). *J. Comp. Neurol.* **432**, 537-549.
Holtmann, M. and Thurm, U. (2001b). Variations of concentric hair cells in a cnidarian sensory epithelium (*Coryne tubulosa*). *J. Comp. Neurol.* **432**, 550-563.
Johnston, D. and Wu, S. M.-S. (1995). *Foundations of Cellular Neurophysiology*, pp. 369, 392-395. London: MIT Press.
Kass-Simon, G. and Pierobon, P. (2007). Cnidarian chemical neurotransmission, an updated overview. *Comp. Biochem. Physiol. A* **146**, 9-25.
Kass-Simon, G. and Scappaticci, A. A., Jr (2004). Glutamatergic and GABAnergic control in the tentacle effector systems of *Hydra vulgaris*. *Hydrobiologia* **530/531**, 67-71.
Katz, B. and Miledi, R. (1967). The timing of calcium action during neuromuscular transmission. *J. Physiol.* **189**, 535-544.
Kerfoot, P. A. H., Mackie, G. O., Meech, R. W., Roberts, A. and Singla, C. L. (1985). Neuromuscular transmission in the jellyfish *Aglantha digitale*. *J. Exp. Biol.* **116**, 1-25.
Lawonn, P. (1999). Die rezeptorischen und effektorischen Funktionen der Nesselzellen von *Hydra vulgaris* und ihre sensorische und synaptische Modulation. *Inaugural-Dissertation, Naturwissenschaftliche Fakultät der Universität Münster* 1-187.
Mackie, G. O. (2004). Epithelial conduction: recent findings, old questions, and where do we go from here? *Hydrobiologia* **530/531,** 73-80.
Mire, P., Nasse, J. and Venable-Thibodeaux, S. (2000). Gap junctional communication in the vibration-sensitive response of sea anemones. *Hear. Res.* **144**, 109-123.
Murphey, A. D., Hadley, R. D. and Kater, S. B. (1983). Axotomy-induced parallel increases in electrical and dye coupling between identified neurons of *Heliosoma*. *J. Neurosci.* **3**, 1422-1429.
Neher, E. (1993). Secretion without full fusion. *Nature* **363**, 497-498.
Nüchter, T., Benoit, M., Engel, U., Özbek, S. and Holstein, T. W. (2006). Nanosecond-scale kinetics of nematocyst discharge. *Curr. Biol.* **16**, R316-R318.
Pantin, C. F. A. (1942). The excitation of nematocysts. *J. Exp. Biol.* **19**, 294-310.
Parker, G. H. (1916). The effector systems of actinians. *J. Exp. Zool.* **21**, 461-484.
Price, R. B. and Anderson, P. A. V. (2006). Chemosensory pathways in the capitate tentacles of the hydroid *Cladonema. Invert. Neurosci.* **6**, 23-32.
Purcell, J. E. and Anderson, P. A. V. (1995). Electrical responses to water-soluble components of fish mucus recorded from the nematocytes of a fish predator, *Physalia physalis*. *Mar. Fresh. Behav. Physiol.* **26**, 149-162.
Shibayama, J., Paznekas, W., Seki, A., Taffet, S., Jabs, E. W., Delmar, M. and Musa, H. (2005). Functional characterization of connexin43 mutations found in patients with oculodentodigital dysplasia. *Circ. Res.* **96**, e83-e91.
Sieger, T. and Thurm, U. (1997). Glutamatergic properties of synaptic transmission of the hair-cell-analog nematocytes of Corynidae polyps and their modulation by choline-derivatives. *Göttingen Neurobiol. Report* **1997**, 736.
Slautterback, D. B. (1967). The cnidoblast-musculoepithelial cell complex in the tentacles of Hydra. *Z. Zellforschg.* **79**, 296-318.
Spencer, A. N. (1982). The physiology of a coelenterate neuromuscular synapse. *J. Comp. Physiol.* **148**, 353-363.
Tardent, P. (1995). The cnidarian cnidocyte, a high-tech cellular weaponry. *BioEssays* **17**, 351-362.
Thurm, U. and Lawonn, P. (1990). Die sensorischen Eigenschaften des Cnidocil-Apparates als Grundlage des Beutefangs der Hydropolypen. *Verh. Dtsch. Zool. Ges.* **83**, 431.
Thurm, U., Brinkmann, M., Golz, R., Lawonn, P. and Oliver, D. (1998a). The supramolecular basis of mechanoelectric transduction studied in concentric hair bundles of invertebrates. In *From Structure to Information in Sensory Systems* (ed. C. Taddei-Ferretti, and C. Musio), pp. 228-236. Singapore, New Jersey, London, Hong Kong: World Scientific Publishing.
Thurm, U., Brinkmann, M., Holtmann, M., Lawonn, P., Oliver, D. and Sieger, T. (1998b). Modulation of the output of a mechanosensory cell by chemosensory and synaptic inputs. *In From Structure to Information in Sensory Systems* (ed. C. Taddei-Ferretti and C. Musio), pp. 237-253. London: World Scientific Publishing.
Thurm, U., Brinkmann, M., Golz, R., Holtmann, M., Oliver, D. and Sieger, T. (2004). Mechanoreception and synaptic transmission of hydrozoan nematocytes. *Hydrobiologia* **530/531**, 97-105.
Vyshedskiy, A. and Lin, J.-W. (1998). Change of treansmitter release kinetics during facilitation revealed by prolonged test pulses at the inhibitor of the crayfish opener muscle. *J. Neurophysiol.* **78**, 1791-1799.
Vyshedskiy, A., Delaney, K. R. and Lin, J.-W. (1998). Neuromodulators enhance transmitter release by two separate mechanisms at the inhibitor of crayfish opener muscle. *J. Neurosci.* **18**, 5160-5169.
Waldeck, R. F., Pereda, A. and Faber, D. S. (2000). Properties and plasticity of paired-pulse depression at a central synapse. *J. Neurosci.* **20**, 5312-5320.
Watson, G. M. and Hessinger, D. A. (1989). Cnidocytes and adjacent supporting cells form receptor-effector complexes in anemone tentacles. *Tissue Cell* **21**, 17-24.
Westfall, J. A. (1996). Synapses in the first-evolved nervous systems. *J. Neurocytol.* **25**, 735-746.

Table S1. Morphological and electrical characteristics of nematocytes and characteristic data of L- and T-potentials

	Stauridiosarsia producta		*Coryne tubulosa*	*Dipurena reesi*
	Large cells	Small cells		
Size of cell soma (length, diameter; μm)	35, 22	18, 12	16–23, 10–16	~20, 12
Membrane resistance (MΩ)	31±14 (*N*=40)	50.8±19.6 (*N*=6)	35.6±12.4 (*N*=30)	33±10 (*N*=22)
Resting potential (mV)	Series 1: –58±13.3 (*N*=137) Series 2: –53.4±18.8 (*N*=78)		53.8±15.2 (*N*=34)	53±13 (*N*=53)
L-potentials (L-EPSP) at stimulation of distant nematocytes	Large cells			
	Without distant cyst-discharge*	With distant cyst-discharge*		
Amplitude (mV)	1–24 (*N*=164)	10–44 25±6.2 (*N*=146)	n.d.	38±4 (*N*=12)
Duration of 90% rise (ms)	5.2–24	2.5–7	n.d.	88±20 (*N*=12)
Duration at half amplitude of single peak (ms)	36–250	61–300	n.d.	66±30 (*N*=12)
Duration of decay (ms)	80–550	>500	n.d.	552±266 (*N*=12)
Latency (ms)	2.6-45 (*N*=164)	0.6-10.7 2.1±1.2 (*N*=146)	n.d.	93±6 (*N*=12)
Latency at stimulation of hair cells (ms)	9–100		13–98	n.d.
T-potentials, depolarizing component (T-EPSP)				
Amplitude (mV) (non-repetitive potentials)	20–45		⩽55	29±5 (*N*=9)
Duration of 90% rise (ms)	8–80 (incl. smooth start, see Fig. 4C 2)		n.d.	5±1.4 (*N*=9)
Duration at half amplitude of single peak (ms)	5–32 24±7 (*N*=6)		3–5	5.7±1.4 (*N*=9)
Duration of decay (ms)	~100		n.d.	n.d.
Latency at mech. stimulation of tentacular shaft (ms)	30–100		n.d.	n.d.
T-potentials, hyperpolarizing component (T-IPSP)				
Prevalence	8% of cells		100% of cells	100% of cells
Amplitude (non-repet. pot.) (mV)	–3		–11	–8
Duration at half amplitude (ms)	~100		40–50	40–120

*Most of the stimuli that did not evoke discharge of the stimulated nematocyte were purely mechanical; stimuli that evoked a discharge were mostly chemo-mechanical (see text). n.d.: not determined